Analysis and Prediction of the Freezing of Gait Using EEG Brain Dynamics

A. M. Ardi Handojoseno, *Student Member, IEEE*, James M. Shine, Tuan N. Nguyen, *Member, IEEE*, Yvonne Tran, Simon J. G. Lewis, and Hung T. Nguyen, *Senior Member, IEEE*

***Abstract*—Freezing of Gait (FOG) is a common symptom in the advanced stages of Parkinson's disease (PD), which significantly affects patients' quality of life. Treatment options offer limited benefit and there are currently no mechanisms able to effectively detect FOG before it occurs, allowing time for a sufferer to avert a freezing episode. Electroencephalography (EEG) offers a novel technique that may be able to address this problem. In this paper, we investigated the univariate and multivariate EEG features determined by both Fourier and wavelet analysis in the confirmation and prediction of FOG. The EEG power measures and network properties from 16 patients with PD and FOG were extracted and analyzed. It was found that both power spectral density and wavelet energy could potentially act as biomarkers during FOG. Information in the frequency domain of the EEG was found to provide better discrimination of EEG signals during transition to freezing than information coded in the time domain. The performance of the FOG prediction systems improved when the information from both domains was used. This combination resulted in a sensitivity of 86.0%, specificity of 74.4%, and accuracy of 80.2% when predicting episodes of freezing, outperforming current accelerometry-based tools for the prediction of FOG.**

***Index Terms*—Biomedical signal processing, electroencephalogram, freeing of gait (FOG), movement disorders, Parkinson's disease (PD).**

I. Introduction

FREEZING of gait (FOG) is a highly disabling symptom that affects approximately one quarter of patients with Parkinson's disease (PD) in the early stages and over two thirds in the advanced stages of the disease [1]. Clinically, FOG is defined as a *"brief, episodic absence or marked reduction of forward progression of the feet despite the intension to walk"* [2]. Balance impairment and falls due to sudden FOG often develop into one of the chief complaints among patients with PD and also often lead to falls, which are associated with a high morbidity and mortality in PD [3].

Manuscript received April 07, 2014; revised September 13, 2014, November 03, 2014; accepted November 23, 2014. Date of publication December 18, 2014; date of current version September 03, 2015.

A. M. Ardi Handojoseno, Tuan N. Nguyen, and Hung T. Nguyen are with Faculty of Engineering and Information Technology, University of Technology, Sydney, NSW 2007, Australia (e-mail: aluysiusmariaardi.handojoseno@student.uts.edu.au; tuannghia.nguyen@uts.edu.au; hung.nguyen@uts.edu.au).

J. M. Shine and S. J. G. Lewis are with Parkinson's Disease Research Clinic, Brain and Mind Research Institute, University of Sydney, Camperdown, NSW, 2050, Australia(e-mail: mac.shine@sydney.edu.au, simonl@med.usyd.edu.au).

Y. Tran is with the Centre for Health Technologies, University of Technology, Sydney , NSW 2007, Australia, and also with the Rehabilitation Studies Unit, University of Sydney, Sydney, NSW 2007, Australia (e-mail: yvonne.tran@uts.edu.au).

Digital Object Identifier 10.1109/TNSRE.2014.2381254

The manifestation of FOG is intimately related to the external environment of the individual. Several specific scenarios have been found to initiate FOG, including dual tasking, passing through doorways or crowded areas, as well as stress and anxiety. Together, the multifactorial nature of these triggers indicates a multisystem deficit in FOG, in which impaired information processing across cognitive, affective, and motor domains leads to overwhelming inhibition over the brainstem structures that control gait [4], [5]. This proposal has been supported by the results of functional neuroimaging [6]–[8].

Since dopaminergic replacement therapy only partially alleviates FOG, different strategies have been developed to trigger alternative neural circuits in behavioral control. Somatosensory cues have been found to improve walking, with visual cues offering the strongest influence, followed by tactile, emotional, and auditory cues [9]. A recent investigation on the effect of visual cues using laser on seven PD patients with FOG showed that on-demand cueing (only given when FOG episodes were observed) is more efficient for reducing the duration of FOG periods than continuous cueing [10], which indicates the importance of a FOG detection system.

While various methods have been investigated to detect the onset of freezing, none of these techniques seem able to reliably detect FOG [11]–[15]. To predict the onset of freezing at the earliest time before the actual FOG episodes, as oppose to detection, we have used EEG due to its ability to measure dynamic physiological change in the brain prior to the occurrence of movement disturbances. Using EEG, both cortical and subcortical activity can be studied through the time-varying changes in certain spectral bands, which also allow insights into the mechanism of FOG. Finally, the portability and relative ease of use of EEG make it far more useful for the mobile collection of brain activity data.

Wavelet decomposition based features have been developed and show the potential of EEG signals as a bio-marker for detecting FOG [16]. In this study, we attempted to find highly discriminating features by investigating the performance of Fourier-based features and their counterpart in the wavelet domain, and the performance of univariate and bivariate EEG measurements in detecting FOG in PD patients. Two inter-related categories of EEG measurement were examined: power or amplitude measures and EEG network properties, which may also disclose critical aspects of the functional connectivity of neural networks during a freezing episode. Some classic features such as power spectrum, centroid frequency, and statistical parameters were also computed, as well as more recently developed features such as entropy, cross correlation,

coherence, phase-locking value, and weighted phase lag index. Multilayer perceptron neural networks (MLP-NN) classifier was employed for FOG detection, concentrating on the transition period between normal walking and an overt FOG episode.

II. Methods

The study included 16 patients ranging in age from 56 to 78 years (mean: 64 years, std: 7.25 years) with the mean Hoehn and Yahr stage when "off" medications over night was 2.34 ± 0.73 and the mean of the Unified Parkinson's Disease Rating Scale III stage when "off" was 40.10 ± 12.21. All of them had a FOG history with different severity and frequency. The research protocol was approved by The Human Research and Ethics Committee from the University of Sydney before data collection began. The experiment took place in the Parkinson's Disease Research Clinic at the Brain and Mind Research Institute, University of Sydney during a one week period. A series of a standardized timed up-and-go tasks were performed and all trials were video recorded for scoring.

Several researchers have shown that information on EEG signals relating to mental tasks or the physiological condition can be tracked using only a minimum points of measurement [17], [18]. Fewer channels are clearly preferred for patient ease and to limit noise and artifacts. Moreover, it reduces the cost in signal processing, feature extraction and classification process; and makes the setting up of the system much easier and faster.

In this study, the EEG was recorded using a 4-channel wireless EEG system with gold cup electrodes which were placed on four scalps locations based on their roles in perceptual and control movement (O1-visual, P4-sensorimotor affordance, Cz-motor execution, and Fz-motor planning). Bipolar EEG leads were used to acquire data from central zero (Cz) and frontal zero (Fz) with the reference electrode placed at FCz, and from occipital one (O1) and parietal four (P4) with the reference electrode at T4 and T3, respectively. The EEG signals were amplified with common rejection ratio >95 dB, sampled at a rate of 500 Hz, and band-pass filtered between 0.15 and 100 Hz.

Overall 5.5 h of data were collected from the standardized timed up-and-go test and 404 FOG episodes, with a duration between 1 s and 220 s, were labeled by two clinicians specializing in movement disorders. Two other episodes were determined based on this period: transition episodes which cover a period between 5 to 1 s before freezing, and normal walking which refers to a period of 1 s after freezing to 5 s before the next freezing period. The distribution of FOG among the patients were not equal: three patients had between 6 and 10 episodes during testing and the remaining 13 patients experienced more than 10 events. A total of 1902 1-s duration samples of three episodes (normal walking, transition, FOG) from all patients were included with each episode contributed evenly (634 samples). Data from eleven patients were randomly chosen for training and testing (consisting of 1386 samples, 462 in each class). Another set of testing data files, which have never been used in the training process, were also taken from the other five patients (516 samples, 172 in each class) to examine the robustness of the system in classifying the EEG signals from out-group patients. Low frequency noise, high frequency noise and 50 Hz line frequency noise were eliminated using band-pass (0.5–60 Hz) and band-stop (50 Hz) Butterworth IIR filters. Ocular and muscular artifacts were removed using Stein's unbiased risk estimate thresholding based on wavelet transforms.

III. Feature Extraction

A. EEG Linear Univariate Measurements

Power spectral density (PSD), which is widely used and successfully applied to characterize signals in a system, shows the strength of the energy as a function of frequency. It implies stationary process during the time window. While EEG signals are known as nonstationary signals with nonlinear behavior [19], fragments of EEG with length up to 290 ms can be treated as stationary [20].

In this study, the spectra are calculated via Welch's method using a 516 point fast Fourier transform (FFT) and periodic Hamming windows with an overlap of 50%. The duration of the stationary fragments is assumed to be 110 ms with the sampling frequency 500 Hz. To eliminate inter-individual and inter-electrode variance in absolute measurements, the power spectrum was normalized by expressing each power spectral as a percentage of total power in a frequency window of 0.5–60 Hz and in all electrodes. EEG bands of interest were delta (1–4 Hz), theta (4–8 Hz), alpha (8–13 Hz), beta (13–30 Hz), and gamma (30–60 Hz).

Furthermore, we calculate the shift of the center of gravity of frequency band based on this normalized power spectrum, Spectral Centroid Frequency (SCF). It has been reported to be capable of classifying different types of EEG in various health conditions [21], [22] and is defined as

$$\mathrm{SCF} = \frac{\sum_i f_i * P(f)}{\sum_i P(f)}. \tag{1}$$

Over the past few decades, wavelet analysis has been developed as an alternative and improvement on Fourier analysis. Its main advantage in analyzing physiological systems is its capability to detect and analyze nonstationarity in signals and its related aspect like trends, breakdown points, and discontinuity, since wavelets are well localized in both time and frequency domain. Unlike Fourier transform which is limited to a scaled single sinusoidal function, wavelet transform generates a two-parameter family of wavelet function $\psi_{a,b}(t)$ by scaling (a) and shifting (b) the function, so that the correlation called continuous wavelet transform (CWT) is given by [23]

$$\mathrm{CWT}(a,b) = \int_{-\infty}^{\infty} x(t) \frac{1}{\sqrt{|a|}} \psi^* \left(\frac{t-b}{a} \right) dt \tag{2}$$

with $^{(*)}$ denotes the complex conjugation.

The development of wavelet-based signal compression algorithm led to the invention of the fast discrete wavelet transforms (DWT) which removes redundancy in the signals and simplify the numerical calculations. In DWT time-scaled parameters (b, a) are sampled on a dyadic grid with scales $a = 2^j$

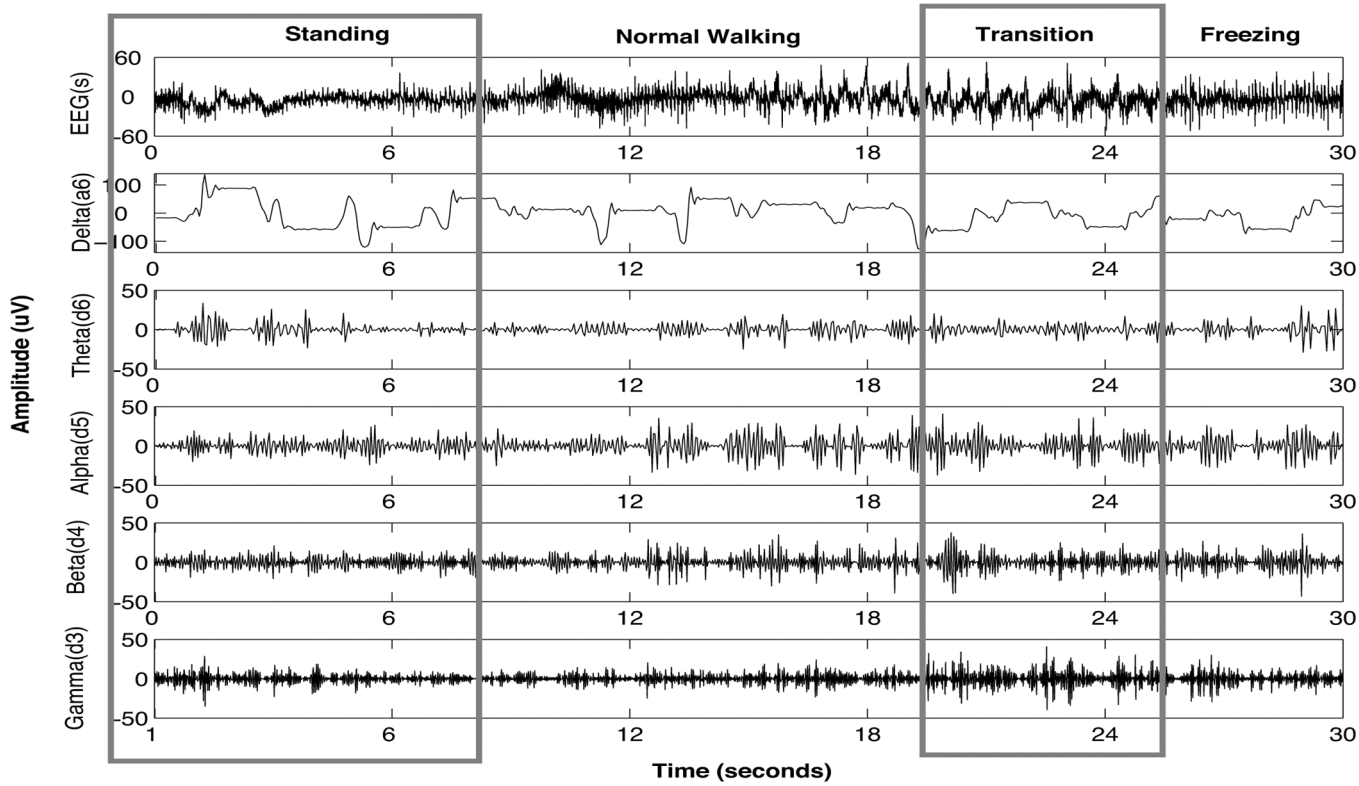

Fig. 1. Decomposition of EEG into detail (d1–d5) signals related to five standard clinical EEG subbands by db4 wavelet in subject 6 shows the amplitude and frequency alterations preceding and during freezing episode. Movement amplitude is increased preceding the freezing episode.

(reciprocal of frequency) and positions $b = 2^j k$ (time localization), so that DWT is defined as

$$\mathrm{DWT}(j,k) = \frac{1}{\sqrt{|2^j|}} \sum_{t=-\infty}^{\infty} x(t)\psi\left(\frac{t-2^j k}{2^j}\right). \quad (3)$$

In the multiresolution analysis, signal $x(t)$ with maximum cut-off frequency f_m is split into two components using low pass filter and high pass filter and is down sampled by 2 to provide the approximation signals A_j and the detail signals D_j with lower cut-off frequency band $[0 : f_m/2]$ and upper cut-off frequency band $[f_m/2 : f_m]$, respectively [24]. Based on the Nyquist criterion, maximum cut-off frequency is determined by $f_m = f_s/2^{(l+1)}$ where f_s is the sampling frequency of the original signal and l is the level of decomposition. The approximation is subsequently decomposed and this process is continued until the target level is achieved.

The wavelet decomposition for a given EEG signal $x(t)$ at scales $j = 1, 2, \ldots, J$ and time point k then could be written as

$$x(t) = \sum_k c_{J,k}\varphi_{J,k}(t) + \sum_k \sum_{j\le J} d_{j,k}\psi_{j,k}(t) \quad (4)$$

where $c_{J,k}$, $d_{j,k}$, $\varphi_{j,k}(t)$, and $\psi_{j,k}(t)$ are the approximation coefficients, the detail coefficients, scaling function, and wavelet functions, respectively. Daubechies (db4) wavelet that has been found as properly representing EEG signals and spikes [25] was selected as wavelet function.

With the EEG sampled at 500 Hz, a good match to the standard clinical EEG subbands can be achieved using a six level decomposition as can be seen in Table I. Reconstruction of these signals which are decomposed into five constituent EEG subbands is depicted in Fig. 1.

TABLE I
FREQUENCY BANDS CORRESPONDING TO DIFFERENT DECOMPOSITION LEVELS

Decomposed signals	Frequency bands (Hz)	Decomposition Level
D1	125-250	1 (noises)
D2	62.5-125	2 (noises)
D3	31.3-62.5	3 (γ)
D4	15.6-31.3	4 (β)
D5	7.8-15.6	5 (α)
D6	3.9-7.8	6 (θ)
A6	0-3.9	6 (δ)

In wavelet analysis, the energy of signals which correspond to PSD, wavelet energy (WE), can be partitioned at different levels of wavelet decomposition ($j = 1, \ldots l$) according to Parseval's Theorem, and is expressed as a function of the scaling and wavelet coefficient [26]

$$E_T = \int |f(t)|^2\, dt = \sum_k |c_{J,k}|^2 + \sum_k \sum_{j\le J} |d_{j,k}|^2. \quad (5)$$

Corresponding to SCF, we also calculated Centroid Scale (CS) based on the CWT scalogram to show the shift of the center of gravity of frequency band. The CWT was chosen since it has a better frequency (scale) representation compared to the DWT. We used the complex Morlet wavelet due to its narrow spectral band and an extended time domain made it more suitable for extracting information in frequency domain [27]. It is equivalent to a complex sinusoid with Gaussian envelope and can be written as [28]

$$\psi_0(t) = \frac{1}{\sqrt[4]{\pi}} e^{j2\pi f t} e^{-\frac{t^2}{2}}. \quad (6)$$

B. EEG Nonlinear Univariate Measurements

Brain signals have been known as the output of a nonlinear system. Consequently, various measures which characterize the nonlinear behavior of EEG signals have also been developed. In this study, entropy was used as an index of EEG complexity or irregularity based on Shannon's Information Theory. The power spectral entropy (PSE) of EEG signal x is defined as

$$\mathrm{PSE}(x) = -\sum_{i=f_l}^{f_h} P_i \log P_i \tag{7}$$

where P_i is the normalized power density from the signal's spectrum so that $\sum P_n = 1$ while f_l and f_h are the frequency band of interest. Larger entropy values suggest a greater complexity. The wavelet energy entropy (WEE) were found using similar formula, with

$$P_i = \frac{E_j}{E_T} \tag{8}$$

in which E_j refers to the energy of signals at jth frequency band of decomposition and E_T refers to the energy of all frequency bands of decomposition.

C. EEG Bivariate Measurements

There is a growing interest in the study of oscillatory rhythms and their synchronization related to the dynamic organization of communication in the nervous system. They have been associated with diverse functions such as motor activity, attention, memory, and emotion. This was obtained by joining signals from multiple channels to detect the alteration of the functional connectivity in the brain related to different brain conditions.

In this study, quantification of neural correlation was done based on the cross-correlation function, defined as [30]

$$R_{xy}(k) = E[x(n)y(n+k)] \tag{9}$$

where $x(n)$ and $y(n+k)$ are two joint signals, k is the number of time units that the signal $y(n)$ is lagged in regards to $x(n)$, and $E[\cdot]$ is the expectation operator.

Cross power spectral density (CPSD) as the distribution of power per unit frequency is defined as

$$P_{xy}(f) = \sum_{k=-\infty}^{\infty} R_{xy}(k) e^{-j2\pi fkT}. \tag{10}$$

Ratio of CPSD to the product of the related auto-power spectral densities (APSD) shows the coherency, a measurement of amplitude and phase coupling, and is defined as

$$C_{xy}(f) = \frac{|P_{xy}(f)|}{\sqrt{P_{xx}(f)P_{yy}(f)}}. \tag{11}$$

Coherency function is a function of frequency and can be used to analyze which frequency of two sets of time series data are coherent. While correlation emphasizes the similarity of waveform between two signals and gives the information on their time coupling, coherency measures the stability of that similarity [31]. Coherence is defined as the modulus of the coherency, also called the magnitude squared coherence (MSC) and typically estimated by averaging over several epochs.

Analysis on the stability of phase shift over the specified time interval also provides measurement of phase difference between two signals. Detecting this phase-locking when the phase difference is constant using correlation and coherence can be problematic since they are affected by the amplitude component which can be noisy or uncorrelated.

Weighted Phase Lag Index (WPLI) was calculated to measure this phase-synchronization. Proposed by Vinck *et al.* [32], it has been demonstrated as reduced sensitivity to noise, increased capacity to detect changes in phase synchronization and is not affected by volume-conducting correlated sources of interest. WPLI is defined as

$$\Phi \equiv \frac{|P\{\Im\{X\}\}|}{P\{|\Im\{X\}|\}} = \frac{|P\{|\Im\{X\}|\mathrm{sgn}(\Im\{X\})\}|}{P\{|\Im\{X\}|\}}. \tag{12}$$

Wavelet analysis has been proposed in estimating the time varying coherence among nonstationary signals including neural signals since FFT is incapable of providing temporal structure information of signals. While a real wavelet function has been used for detecting peaks and discontinuities, information about the difference of phase can only be extracted using a complex wavelet function. Moreover, it is a better method for capturing oscillatory behavior. In this study, we used a complex Morlet wavelet which has been proved provided the best time-frequency resolution in the EEG analysis compared to other wavelet functions [33].

Corresponding to a similar concept in Fourier analysis, the autocorrelation function of the wavelet transformation produces a wavelet power spectrum (WPS) which describes the power of the signals $x(t)$ at a certain time t_i on a scale s

$$\mathrm{WPS}_i(s) = W_i(s)W_i(s)^*. \tag{13}$$

The extension of the univariate WPS to a comparison of two time series x and y at time shift index i and scale s with their wavelet transform coefficients W_{x_i} and W_{y_i}, the wavelet cross spectrum $\mathrm{WCS}_i(s)$, is defined as

$$\mathrm{WCS}_{xy_i}(s) = S\left(W_{x_i}(s)W_{y_i}^{*T}(s)\right) \tag{14}$$

where S is a smoothing operator. The interaction between signals x and y at the given frequency is measured by the product of two spectra expressed by wavelet coefficients of the time scale representation of EEG sub-bands.

Analogous to Fourier-based coherence, wavelet coherence is defined as the amplitude of the WCS normalized to the two single WPS

$$\mathrm{WCO}_{xy_i}(s) = \frac{\mathrm{WCS}_{xy_i}(s)}{\sqrt{S\left(|\mathrm{WPS}_{xx_i}(s)|^2\right)}\sqrt{S|\mathrm{WPS}_{yy_i}(s)|^2}}. \tag{15}$$

To measure phase synchrony based on wavelet transform, Phase Locking Value (PLV) proposed by Lachaux *et al.* [34], which has been also called as mean phase coherence [35], was used in this study, defined as

$$\mathrm{PLV}_t = \frac{1}{N}\left|\sum_{n=1}^{N} N e^{j\theta(t,n)}\right| \tag{16}$$

where $\theta(t,n)$ is the phase difference between the signals which can be derived from the angles of their wavelet-coefficients $\theta_1(t,n) - \theta_2(t,n)$. Just like WPLI, the value of PLV is always between 0 and 1 with a value of 1 signifying perfect synchrony in which one signal perfectly follows the other.

TABLE II
CORRELATION ANALYSIS OF NORMALIZED POWER SPECTRAL DENSITY AND NORMALIZED WAVELET ENERGY BETWEEN NORMAL WALKING (NW) AND TRANSITION TO A FREEZING OF GAIT (TR)

		Power Spectral Density			Wavelet Energy		
Lead	Frequency	NW	TR	NW vs TR	NW	TR	NW vs TR
O1	δ	0.0868 ± 0.0595	0.0816 ± 0.0743	*	0.0051 ± 0.0094	0.0082 ± 0.0373	*
	θ	0.0872 ± 0.0565	0.0814 ± 0.0716	*	0.0005 ± 0.0012	0.0003 ± 0.0007	*
	α	0.0643 ± 0.0361	0.0575 ± 0.0459	*	0.0007 ± 0.0018	0.0004 ± 0.0029	**
	β	0.0691 ± 0.0375	0.0426 ± 0.0252	***	0.0005 ± 0.0017	0.0004 ± 0.0032	***
	γ	0.0415 ± 0.0330	0.0160 ± 0.0159	**	0.0003 ± 0.0012	0.0007 ± 0.0081	***
P4	δ	0.1436 ± 0.0837	0.0920 ± 0.0652	**	0.0133 ± 0.0536	0.0068 ± 0.0333	**
	θ	0.1456 ± 0.0770	0.0949 ± 0.0632	**	0.0007 ± 0.0019	0.0003 ± 0.0009	*
	α	0.1104 ± 0.0444	0.0750 ± 0.0445	***	0.0013 ± 0.0030	0.0006 ± 0.0041	***
	β	0.1428 ± 0.0711	0.1013 ± 0.0744	***	0.0013 ± 0.0040	0.0005 ± 0.0030	***
	γ	0.1033 ± 0.0827	0.0663 ± 0.0668	*	0.0011 ± 0.0025	0.0006 ± 0.0039	**
Cz	δ	0.0439 ± 0.0552	0.1466 ± 0.1070	***	0.0014 ± 0.0023	0.0052 ± 0.0120	*
	θ	0.0435 ± 0.0536	0.1443 ± 0.1048	***	0.0002 ± 0.0006	0.0008 ± 0.0015	*
	α	0.0301 ± 0.0349	0.0972 ± 0.0699	***	0.0002 ± 0.0004	0.0003 ± 0.0006	
	β	0.0200 ± 0.0158	0.0473 ± 0.0326	***	0.0001 ± 0.0001	0.0001 ± 0.0002	*
	γ	0.0024 ± 0.0022	0.0039 ± 0.0055		0.0000 ± 0.0000	0.0001 ± 0.0009	
Fz	δ	0.0021 ± 0.0025	0.0042 ± 0.0094		0.0001 ± 0.0002	0.0003 ± 0.0016	*
	θ	0.0019 ± 0.0023	0.0040 ± 0.0089		0.0000 ± 0.0000	0.0000 ± 0.0002	
	α	0.0012 ± 0.0014	0.0025 ± 0.0054	*	0.0000 ± 0.0000	0.0000 ± 0.0001	*
	β	0.0003 ± 0.0004	0.0009 ± 0.0017	*	0.0000 ± 0.0000	0.0000 ± 0.0000	*
	γ	0.0000 ± 0.0000	0.0001 ± 0.0006	*	0.0000 ± 0.0000	0.0000 ± 0.0001	*

$* = p \leq 0.05$ and r < 0.3
$** = p \leq 0.05$ and $0.3 \leq$ r < 0.4
$*** = p \leq 0.05$ and r ≥ 0.4

D. Statistical Test and Classification

In order to build a faster and better classification system, we selected the most relevant univariate features using nonparametric statistical analysis—the Wilcoxon Sum Rank Test. Only features with significant statistical differences between those groups of data ($p-$value < 0.05) were chosen for further process.

Classification data sampled using selected features were based on three layers MLP-NN with 56%, 25%, and 19% of the data, randomly split, used for training, validation and testing, respectively. Levernberg-Marquardt algorithm was chosen as a training method for its speed and stability [38]. Known as a combination of the Gauss-Newton technique and the steepest descent method, the Levernberg-Marquardt algorithm essentially is an iterative technique that located the minimum of an objective error function

$$E(w) = \sum_{i=1}^{m} e_i^2(w) = \|f(w)\|^2 \tag{17}$$

where $e_i^2(w) = (y_{di} - y_i)^2$ is an individual error, the difference between the desired value of output neuron y_{di} and the actual output of that neuron, y_i, and w is the weight vector. The Levenberg-Marquardt algorithm is used to find the new weight vector w_{k+1} to reach the optimum performance of the system

$$w_{k+1} = w_k - \left(J_k^T f(w_k)\right)\left(J_k^T J_k + \lambda I\right)^{-1} \tag{18}$$

where J_k is the Jacobian of function $f(\cdot)$ at w_k, λ is the learning rate and I is the identity matrix.

Validation set was used as a stopping criterion to avoid overfitting as well as error goal 0.01 in single MLP-NN with 4–12 hidden layer neurons. Each feature was trained and tested fifty times based on the repeated random sub-sampling and the mean result was recorded. The sensitivity, specificity, accuracy, and area under the receiver operating characteristic curve of classification system were calculated to measure the performance of the features.

IV. RESULTS

A. EEG Linear Univariate Measurements

In the statistical analysis of PSD and WE for differentiation of two EEG conditions, normal walking and transition to FOG, the discriminative value ($p-$value < 0.05) was found in almost all frequency bands as can be seen in Table II. However, when effect size was taken into account, the alpha frequency band in parietal appeared as the most important feature signified with the decreasing of normalized PSD and WE during transition to FOG compared to normal walking (PSD, z $= 7.98$, $p < 0.05$, r $= 0.40$; WE, z $= 8.36$, $p < 0.05$, r $= 0.42$). In addition, there were significant increases in beta power in occipital (PSD, z $= 7.98$, $p < 0.05$, r $= 0.40$; WE, z $= 9.57$, $p < 0.05$, r $= 0.48$), parietal (PSD, z $= 7.98$, $p < 0.05$, r $= 0.40$; WE, z $= 8.87$, $p < 0.05$, r $= 0.45$) and central leads (PSD, z $= 7.98$, $p < 0.05$, r $= 0.40$; WE, z $= 2.63$, $p < 0.05$, r $= 0.13$), along with theta activity in central (PSD, z $= -12.80$, $p < 0.05$, r $= 0.92$; WE, z $= -5.27$, $p < 0.05$, r $= 0.27$).

Common patterns shared by Fourier transform based features and wavelet transform based features clearly showed in the shifting centroid frequency in the beta, alpha, and theta frequency band during transition and freezing episodes. The beta frequency band stands out as the most affected frequency band in transition to freezing with the most significant shift

happening in the central lead (SCF, $z = 11.04$, $p < 0.05$, $r = 0.56$; CS, $z = -8.33$, $p < 0.05$, $r = 0.42$) while the fronto-central cortical region has been more affected than the parieto-occipital region. When compared to the walking period, episodes of freezing were associated with significant shifting in the theta frequency band with the largest shift of centroid frequency in the frontal leads (SCF, $z = -4.11$, $p < 0.05$, $r = 0.21$; CS, $z = 4.55$, $p < 0.05$, $r = 0.23$).

B. EEG Nonlinear Univariate Measurements

The result of entropy analysis shows a decrease of entropy in most frequency bands and electrodes during freezing of gait. The most significant change during transition to freezing was detected in the beta frequency band both at central (PSE, $z = 11.01$, $p < 0.05$, $r = 0.56$) and frontal (PSE, $z = 8.23$, $p < 0.05$, $r = 0.42$). This trend was continued in the onset of freezing with lower effect size (Central: PSE, $z = 4.35$, $p < 0.05$, $r = 0.22$; Frontal: PSE, $z = -5.44$, $p < 0.05$, $r = 0.28$).

The entropy analysis on wavelet energy which measures the temporal regularity of energy in each frequency band also revealed the loss of complexity during transition in most of all the frequency bands and electrodes with the beta band appearing as the most affected frequency band. There was a significant decreased regularity of gamma activity in the central (WEE, $z = 11.04$, $p < 0.05$, $r = 0.56$) during the transition, along with a decrease in the beta band (WEE, $z = 11.04$, $p < 0.05$, $r = 0.56$). While these entropy were then increased at the onset of the freezing period, they were still significantly lower compared to walking, unlike the diminishing of all irregularity at the occipital and parietal leads.

C. EEG Bivariate Measurements

Fig. 2 shows the results from the phase synchrony analysis obtained from electrodes pairs in three mid-high frequency bands during freezing of gait. Both parietal-frontal and occipital-frontal cortices connections in the beta and gamma frequency band are strongly synchronized in phase according to WPLI analysis. In contrast, when PLV analysis was applied, phase synchronization decreased significantly in the gamma frequency band in both pairs of electrodes location.

In the coherency analysis, both MSC and WCO indicated a significantly different coherency during transition to freezing in parieto-occipital pairwise of electrodes in the theta, alpha and beta frequency band, as illustrated in Figs. 3 and 4. We observed no significant change of coherency in parietal-central cortices connection. Pairwise fronto-central shows alteration of coherence in all frequency bands detected using WCO and in three lowest band frequency using MSC. Amongst all the changes, the most significant one is in the theta frequency band at this pairwise of electrode (MSC, $z = -8.11$, $p < 0.05$, $r = 0.41$; WCO, $z = -5.05$, $p < 0.05$, $r = 0.26$).

D. Statistical Test and Classification

The performance of features extracted through univariate analysis is generally stronger than bivariate analysis based features. Both sub-band power spectrum and sub-band wavelet energy features gave better results compared to their bivariate

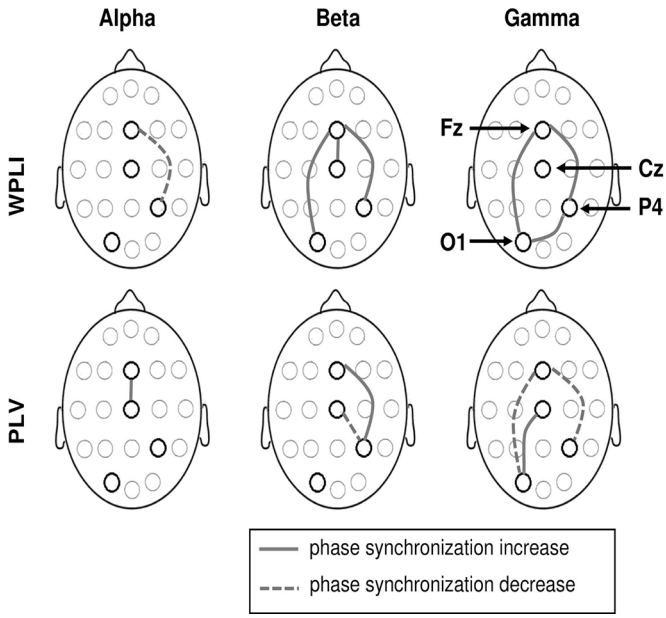

Fig. 2. Phase synchronization alterations during freezing of gait measured using Weighted-Phase Lag Index and Phase Locking Value show the functional link between motor and visual in the high frequency EEG.

mode, cross power spectrum, and wavelet cross spectrum. While our interest is more in the result of in-group testing, since the translation of this method into a real device will be customized for each user due to variation FOG characteristics across patients, it is interesting to point out that the coherence based features poorly performed when it was applied to out-group patients. It shows that multivariate based features are less robust against the inter-individual variability compared to univariate based features.

The result of the experiment also shows that Fourier analysis provided better result compared to wavelet analysis in the extraction of the features related to frequency, entropy, and phase synchrony. However, the changes in the wavelet energy were found to be the best indicators of transition to FOG, with sensitivity and accuracy of testing obtained in the experiment involving in-group patients at 86% and 80.2%, respectively. The using of wavelet cross spectrum also resulted in a better accuracy compared to cross power spectrum in the experiment related to in-group subjects and has been proven as to be more robust when tested against out-group patients, maintaining the accuracy at 77%.

V. Discussion

The present study compared several Fourier analysis based features with their wavelet analysis counter-part and explored their role in neural dynamics related to freezing of gait in PD. Our finding that theta oscillations in human cortex increase during transition to freezing and remain high during freezing in the central region (see Table II-Power Spectral Density) is consistent with multiple studies suggesting that there is a relationship between FOG, specific deficits in cognition and impairment in the motor planning mechanism [39]–[43]. The analysis of the frequency shift and coherency based on MSC and WCO provided more support to the importance of

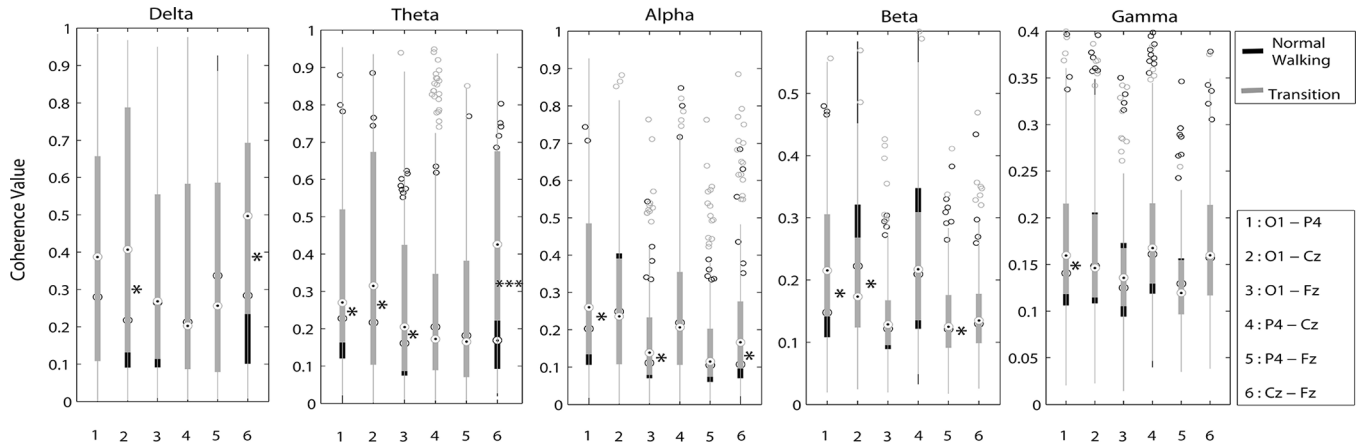

Fig. 3. Boxplot of Magnitude-Squared Coherence of EEG signals during normal walking and transition to freezing of gait (frequency band 5, used electrode 4). Asterisk symbol indicates that the boxplot at its left is significant ($p-\text{value} < 0.05$). Higher number of the asterisk symbol refers to the higher r-value.

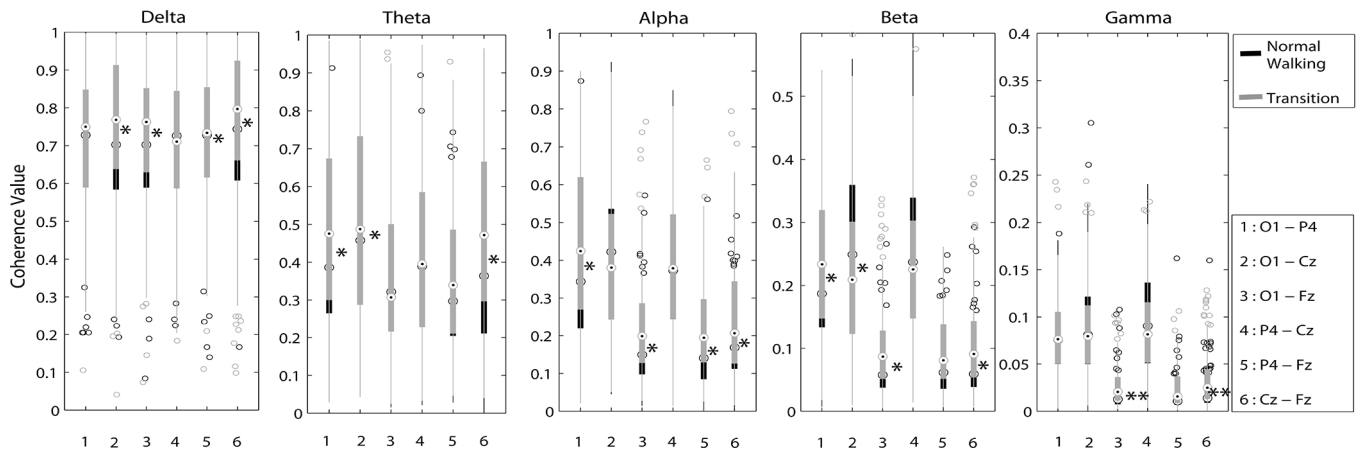

Fig. 4. Boxplot of Wavelet Coherence of EEG signals during normal walking and transition to freezing of gait (frequency band 5, used electrode 4). Asterisk symbol indicates that the boxplot at its left is significant ($p-\text{value} < 0.05$). Higher number of the asterisk symbol refers to the higher r-value.

TABLE III
CLASSIFICATION RESULTS OF PROPOSED FEATURES USING MLP-NN IN DETECTING TRANSITION 5 S BEFORE FREEZING FROM NORMAL WALKING

Features	In-group (11 patients)								Out-group (5 patients)			
	Training				Testing				Testing			
	Se %	Sp %	Ac %	Au %	Se %	Sp %	Ac %	Au %	Se %	Sp %	Ac %	Au %
F1	84.81	84.89	84.83	85.61	79.69	77.98	78.68	79.14	75.86	65.37	70.62	71.52
F2	85.12	82.29	83.67	84.12	81.00	78.96	80.00	79.40	68.51	83.65	76.08	74.53
F3	83.46	82.54	83.00	81.95	79.45	76.94	78.10	79.31	73.02	79.53	76.28	74.30
F4	81.31	81.49	81.71	81.44	74.88	74.76	74.88	75.88	68.40	68.77	68.56	67.42
F5	71.92	77.14	74.58	74.86	70.75	71.73	70.75	69.41	66.16	72.88	68.42	67.23
F6	63.70	80.43	72.10	71.06	64.20	81.22	72.88	71.18	54.88	87.09	70.99	69.04
F7	89.28	78.21	83.75	83.55	86.00	74.43	80.20	79.73	73.19	80.16	76.67	75.88
F8	85.82	80.82	83.29	83.54	79.35	73.81	76.47	75.75	68.77	76.98	72.87	71.27
F9	77.51	73.19	75.29	75.46	71.53	67.00	69.32	70.10	75.09	67.05	71.07	70.14
F10	78.73	87.22	83.00	84.66	72.76	82.89	77.42	77.20	69.93	85.16	77.55	77.80
F11	75.66	78.88	78.67	77.54	66.33	67.71	69.42	68.51	57.51	53.72	52.16	52.37
F12	70.02	74.15	72.07	72.31	60.80	66.13	62.47	61.41	73.07	54.42	52.13	52.52

Se: Sensitivity; Sp: Specificity; Ac: Accuracy; Au: Area under the Receiver Operating Characteristic curve
F1: Power Spectral Density (PSD); F2: Spectral Centroid Frequency (SCF); F3: Power Spectral Entropy (PSE)
F4: Cross Power Spectral Density (CPSD); F5: Magnitude-Squared Coherence (MSC)
F6: Weighted Phase Lag Index (WPLI); F7: Wavelet Energy (WE)
F8: Centroid Scale (CS); F9: Wavelet Energy Entropy (WEE)
F10: Wavelet Cross Spectrum (WCS); F11: Wavelet Coherence (WCO); F12: Phase-Locking Value (PLV)

frontocentral activity in FOG (see Figs. 3 and 4 in which the frontocentral pairwise is significant in most of all frequency bands).

The entropy analysis of the frequency domain based on the changing of power spectral shows an increase of regularity on nearly all frequency bands and most electrodes during transi-

tion and this continued in the freezing period. Therefore we can infer that brain activity is "less complex" when patients undergo change from their normal walking state to freezing of gait. The alteration in the information processing during this stage is possibly due to an inactivation of previously active neural networks as a result of the impairment of the more "executive" functions of the brain. This result is also aligned with the general "loss of complexity" behavior in other diseases and states of the brain including epilepsy [44], Alzheimer's [45], and autism [46].

While there are clear differences in the result of phase synchrony calculation using WPLI and PLV, both are in agreement with the increase of beta synchronization. This result is aligned with the work of Heinrichs-Graham *et al.* [47] who used magnetoencephalography (MEG) and found beta desynchronization prior to and during movement onset as well as increased gamma activity in Parkinson's disease. The analysis on the primary motor cortex arm area by Hemptinne *et al.* [48] also found the exaggerated coupling between beta-phase and gamma amplitude in those areas in PD patients. This coupling has been reported in relation to movement preparation and control of different cognitive functions including memory and attention. Interestingly, we also noticed the significant coherence in the gamma frequency band at pairwise O1-Cz and Cz-Fz, detected using wavelet coherence.

The comparison between power spectral entropy based on the signals dynamic in the frequency domain and wavelet energy entropy based on the signals dynamic in the time domain revealed that information of EEG signals are coded in the frequency domain rather than in the time domain. Along with the results of classification using centroid frequency and centroid scale, it shows that Fourier analysis provides better features in frequency domain compared to wavelet analysis. This precision on frequency, following the Heisenberg Uncertainty Principle, is at the cost of zero information about the temporal dynamic of the signal.

The wavelet analysis provides information on time localization which has increased the performance of the classification system as is shown in the result of wavelet energy. However, in the time-space correlation and coherence, the performance of features extracted using the windowed Fourier transform and the wavelet transform were comparable, with the computation time taken by CWT found to be significantly longer than the windowed Fourier transform. This limits the practical uses of CWT in practical application.

Wearable systems for the detection of FOG episodes have been developed using accelerometers as the main sensor with the sensitivity exceeding 80% [14], [15], [49], [50]. However, unlike the detection system with EEG, those results were acquired in identifying the onset once FOG appeared. Moreover, due to dependency to the physical movement of the body, accelerometers could not differentiate between freezing and voluntarily stopping [51]. EEG has the potential to be an effective means for the prediction of FOG in our study, with sensitivity and accuracy around 80% using power spectral or wavelet energy as a single feature. Besides, there is a possibility to increase the transition period to provide enough window time for signal processing as well as a follow up treatment.

VI. Conclusion

This study demonstrated the potential of the EEG features extracted using both Fourier and wavelet analysis in giving more insights into the pathophysiology of Freezing of Gait in PD. Results also show the advantage of using wavelet analysis in extracting EEG basic feature, energy, compared to Fourier analysis, providing a better indicator in classification system. This finding may be due to its representation of signals in three dimensions (amplitude, frequency, and time) compared to Fourier (amplitude and frequency), which is more convenient for nonstationary EEG signals. However, it was less differentiated in coherency and phase synchrony, when computation of the Fourier coefficients were done in a short time window shifting through the time line, capturing the entire time-frequency of the signals.

Different aspects of the EEG signal, when combined, may provide more significant information, leading to a better classification of the signal. Future work will include dimension reduction of the features highlighted, further exploration regarding the location of electrodes, and investigating different classification methods for better performance of the system. It is hoped that such approaches may lead to clinical translation with device capable of sufficient computational cost and time processing.

References

[1] D. M. Tan, J. L. McGinley, M. E. Danoudis, R. Iansek, and M. E. Morris, "Freezing of gait and activity limitations in people with Parkinson's disease," *Arch. Physic. Med. Rehab.*, vol. 92, no. 7, pp. 1159–1165, Jul. 2011.

[2] J. G. Nutt *et al.*, "Freezing of gait: Moving forward on a mysterious clinical phenomenon," *Lancet Neurol.*, vol. 10, no. 8, pp. 734–744, Aug. 2011.

[3] B. R. Bloem, J. M. Hausdorff, J. E. Visser, and N. Giladi, "Falls and freezing of gait in Parkinson's disease: A review of two interconnected, episodic phenomena," *Mov. Disord.*, vol. 19, no. 8, pp. 871–884, Aug. 2004.

[4] J. M. Shine, S. L. Naismith, and S. J. G. Lewis, "The differential contributions of motor, cognitive and affective disturbance to freezing of gait in Parkinson's disease," *Clin. Neurol. Neurosurg.*, vol. 115, no. 5, pp. 542–545, May 2013.

[5] A. Nieuwboer and N. Giladi, "Characterizing freezing of gait in Parkinson's disease: Models of an episodic phenomenon," *Mov. Disord.*, vol. 28, no. 11, pp. 1509–1519, Sep. 2013.

[6] A. L. Bartels and K. L. Leenders, "Parkinson's disease: The syndrome, the pathogenesis and pathophysiology," *Cortex*, vol. 45, no. 8, pp. 915–921, Sep. 2009.

[7] J. M. Shine *et al.*, "Abnormal patterns of theta frequency oscillations during the temporal evolution of freezing of gait in Parkinson's disease," *Clin. Neurophysiol.*, vol. 125, no. 3, pp. 569–576, Mar. 2014.

[8] Q. J. Almeida and C. A. Lebold, "Freezing of gait in Parkinson's disease: A perceptual cause for a motor impairment?," *J. Neurol. Neurosurg. Psychi.*, vol. 81, no. 5, pp. 513–518, May 2010.

[9] S. Rahman, H. J. Griffin, N. P. Quinn, and M. Jahanshahi, "The factors that induce or overcome freezing of gait in Parkinson's disease," *Behav. Neurol.*, vol. 19, no. 3, pp. 127–136, 2008.

[10] R. Velik, U. Hoffmann, H. Zabaleta, J. F. M. Masso, and T. Keller, "The effect of visual cues on the number and duration of freezing episodes in Parkinsons patients," in *Proc. IEEE Eng. Med. Biol. Soc. Conf.*, 2012, pp. 4656–4659.

[11] S. T. Moore, H. G. MacDougall, and W. G. Ondo, "Ambulatory monitoring of freezing of gait in Parkinson's disease," *J. Neurosci. Methods*, vol. 167, no. 2, pp. 340–348, Jan. 2008.

[12] M. B. Popovic, M. D. Jovicic, S. Radovanovic, I. Petrovic, and V. Kostic, "A simple method to assess freezing of gait in Parkinson's disease patients," *Braz. J. Med. Biol. Res.*, vol. 43, no. 9, pp. 883–889, Sep. 2010.

[13] A. Delval *et al.*, "Objective detection of subtle freezing of gait episodes in Parkinson's disease," *Mov. Disord.*, vol. 25, no. 11, pp. 1684–1693, Aug. 2010.
[14] M. Bachlin *et al.*, "Wearable assistant for Parkinson's disease patients with the freezing of gait symptom," *IEEE Trans. Inf. Technol. Biomed.*, vol. 14, no. 2, pp. 436–446, Mar. 2010.
[15] S. Mazilu *et al.*, "Online detection of freezing of gait with smartphones and machine learning techniques," in *Proc. 6th Int. Conf. Perv. Comput. Tech. Health.*, 2012, pp. 123–130.
[16] A. M. A. Handojoseno *et al.*, "The detection of freezing of gait in Parkinson's disease patients using EEG signals based on wavelet decomposition," in *Proc. 34th Annu. Int. Conf. IEEE Eng. Med. Biol. Soc.*, 2012, pp. 69–72.
[17] S. Wikström *et al.*, "Early single-channel aEEG/EEG predicts outcome in very preterm infants," *Acta Paediatrica*, vol. 101, no. 7, pp. 719–726, Jul. 2012.
[18] A. Picot, S. Charbonnier, and A. Caplier, "On-line detection of drowsiness using brain and visual information," *IEEE Trans. Syst. Man Cybern. A., Syst. Humans*, vol. 42, no. 3, pp. 764–775, May 2012.
[19] S. Sanei and J. A. Chambers, *EEG Signal Processing*. Hoboken, NJ: Wiley, 2008.
[20] B. Schack and W. Krause, "Dynamic power and coherence analysis of ultra short-term cognitive processes—A methodical study," *Brain Topogr.*, vol. 8, no. 2, pp. 127–136, Dec. 1995.
[21] L. B. Nguyen, A. V. Nguyen, S. H. Ling, and H. T. Nguyen, "An adaptive strategy of classification for detecting hypoglycemia using only two EEG channels," in *Proc. 34th Annu. Int. Conf. IEEE Eng. Med. Biol. Soc.*, 2012, pp. 3515–3518.
[22] T. Staudinger and R. Polikar, "Analysis of complexity based EEG features for the diagnosis of Alzheimer's disease," in *Proc. 33th Annu. Int. Conf. IEEE Eng. Med. Biol. Soc.*, 2011, pp. 2033–2036.
[23] J. L. Semmlow, "Biosignal and biomedical image processing: MATLAB-based applications," in *Signal Process. Commun.*. Boca Raton, FL: CRC Press, 2004, vol. 22.
[24] S. Mallat, *A Wavelet Tour of Signal Processing*. London, U.K.: Academic, 1999.
[25] A. Subasi, "EEG signal classification using wavelet feature extraction and a mixture of expert model," *Exp. Syst. Appl.*, vol. 32, no. 4, pp. 1084–1093, May 2007.
[26] C. S. Burrus, R. A. Gopinath, and H. Guo, *Introduction to Wavelets and Wavelet Transforms: A Primer*. Upper Saddle River, NJ: Prentice-Hall., 1998.
[27] Y. Misiti, G. Oppenheim, and J. M. Poggi, *Wavelets and Their Applications*. Karnataka, India: ISTE, 2007, vol. 330.
[28] P. S. Addison, *The Illustrated Wavelet Transform Handbook: Introductory Theory and Applications in Science, Engineering, Medicine and Finance*. Bristol, U.K.: Taylor Francis, 2002.
[29] C. Torrence and G. P. Compo, "A practical guide to wavelet analysis," *Bull. Am. Meteor. Soc.*, vol. 79, no. 1, pp. 61–78, 1998.
[30] R. Shiavi, *Introduction to Applied Statistical Signal Analysis: Guide to Biomedical and Electrical Engineering Applications*. London, U.K.: Academic, 2010.
[31] M. A. Guevara and M. C. Cabrera, "EEG coherence or EEG correlation?," *Int. J. Psychophysiol.*, vol. 23, no. 3, pp. 145–153, Oct. 1996.
[32] M. Vinck, R. Oostenveld, M. Wingerden, F. Battaglia, and C. Pennartz, "An improved index of phase-synchronization for electrophysiological data in the presence of volume-conduction, noise and sample-size bias," *Neuroimage*, vol. 55, no. 4, pp. 1548–1565, Apr. 2011.
[33] E. Sitnikova, A. E. Hramov, A. A. Koronovsky, and G. van Luijtelaar, "Sleep spindles and spike-wave discharges in EEG: Their generic features, similarities and distinctions disclosed with Fourier transform and continuous wavelet analysis," *J. Neurosci. Methods*, vol. 180, no. 2, pp. 304–316, 2009.
[34] J. P. Lachaux, E. Rodriguez, J. Martinerie, and F. J. Varela, "Measuring phase synchrony in brain signals," *Hum. Brain Mapp.*, vol. 8, no. 4, pp. 194–208, 1999.
[35] F. Mormann, K. Lehnertz, P. David, and C. E. Elger, "Mean phase-coherence as a measure for phase synchronization and its application to the EEG of epilepsy patients," *Physica. D*, vol. 144, no. 3–4, pp. 358–369, 2000.
[36] H. M. Hurtado, L. L. Rubchinsky, K. A. Sigvardt, V. L. Wheelock, and C. T. Pappas, "Temporal evolution of oscillations and synchrony in gpi/muscle pairs in Parkinson's disease," *J. Neurophysiol.*, vol. 93, no. 3, pp. 1569–1584, Mar. 2005.
[37] M. G. Knyazeva *et al.*, "Topography of EEG multivariate phase synchronization in early Alzheimer's disease," *Neurobiol. Aging*, vol. 31, no. 7, pp. 1132–1144, Jul. 2010.
[38] E. D. Übeyli, "Combined neural network model employing wavelet coefficients for EEG signals classification," *Digital Signal Process.*, vol. 19, no. 2, pp. 297–308, Mar. 2009.
[39] B. Suchan, D. Zoppelt, and I. Daum, "Frontocentral negativity in electroencephalogram reflects motor response evaluation in humans on correct trials," *Neurosci. Lett.*, vol. 350, no. 2, pp. 101–104, Oct. 2003.
[40] N. Giladi and J. M. Hausdorff, "The role of mental function in the pathogenesis of freezing of gait in Parkinson's disease," *J. Neurol. Sci.*, vol. 248, no. 1–2, pp. 173–176, Oct. 2006.
[41] G. Yogev-Seligmann, J. M. Hausdorff, and N. Giladi, "The role of executive function and attention in gait," *Mov. Disord.*, vol. 23, no. 3, pp. 329–342, Feb. 2008.
[42] J. M. Shine, A. A. Moustafa, E. Matar, M. J. Frank, and S. J. Lewis, "The role of frontostriatal impairment in freezing of gait in Parkinson's disease," *Front. Syst. Neurosci.*, vol. 7, 2013.
[43] P. Knobl, L. Kielstra, and Q. Almeida, "The relationship between motor planning and freezing of gait in Parkinson's disease," *J. Neurol. Neurosurg. Psych.*, vol. 83, no. 1, pp. 98–101, Jan. 2012.
[44] O. A. Rosso, "Entropy changes in brain function," *Int. J. Psychophysiol.*, vol. 64, no. 1, pp. 75–80, Apr. 2007.
[45] D. Abásolo, J. Escudero, R. Hornero, C. Gomez, and P. Espino, "Approximate entropy and auto mutual information analysis of the electroencephalogram in Alzheimer's disease patients," *Med. Biol. Eng. Comput.*, vol. 46, no. 10, pp. 1019–1028, Oct. 2008.
[46] A. Catarino, O. Churches, S. Baron-Cohen, A. Andrade, and H. Ring, "Atypical EEG complexity in autism spectrum conditions: A multiscale entropy analysis," *Clin. Neurophysiol.*, vol. 122, no. 12, pp. 2375–2383, Dec. 2011.
[47] E. Heinrichs-Graham *et al.*, "Neuromagnetic evidence of abnormal movement-related beta desynchronization in Parkinson's disease," *Cerebral Cortex*, 2013.
[48] C. de Hemptinne *et al.*, "Exaggerated phase-amplitude coupling in the primary motor cortex in Parkinson disease," *Proc. Nat. Acad. Sci.*, vol. 110, no. 12, pp. 4780–4785, Mar. 2013.
[49] Y. Zhao *et al.*, "Online FOG identification in Parkinson's disease with a time-frequency combined algorithm," in *Proc. IEEE-EMBS Int. Conf. Biom. Health Inf.*, 2012, pp. 192–195.
[50] E. E. Tripoliti *et al.*, "Automatic detection of freezing of gait events in patients with Parkinson's disease," *Comput. Meth. Prog. Biom.*, vol. 110, no. 1, pp. 12–26, Apr. 2013.
[51] K. Niazmand *et al.*, "Freezing of gait detection in Parkinson's disease using accelerometer based smart clothes," in *Proc. IEEE Bio. Circ. Syst. Conf.*, 2011, pp. 201–204.

Aluysius Maria Ardi Handojoseno (S'11) received the B.E.E. degree from Sepuluh Nopember Institute of Technology, Surabaya (ITS), Indonesia, and the M.Eng. degree in electrical engineering from the University of Technology, Sydney, Australia, where he has been working toward the Ph.D. degree in electrical engineering in the Centre for Health Technologies, since August 2011.

His current research interests include machine learning and biomedical signal processing with specialization in neurosignal processing.

James Mac Shine is an NHMRC CJ Martin Fellow currently working at Stanford University. Despite being early in his career, he has already made key contributions to the understanding of the pathophysiological mechanisms underlying common, yet poorly understood, symptoms of Parkinson's disease. By using a combination of neuropsychological tasks with advanced analysis of functional brain imaging data, he has published over 40 papers in peer reviewed journals, including many in high-impact international journals. In addition, his work has been highlighted multiple times by the Faculty of 1000. He has over 450 citations and an H-index of 14.

Tuan Nghia Nguyen (M'11) received the Ph.D. degree in engineering from the University of Technology, Sydney, Australia, in 2010.

Currently, he is a Chancellor's Postdoctoral Research Fellow in the Centre for Health Technologies, Faculty of Engineering at the University of Technology, Sydney, Australia. His current research interests include biomedical engineering, advanced control, and artificial intelligence for health technologies.

Dr. Nguyen was awarded as a recipient of the Chancellor's List in recognition of exceptional scholarly achievement in Ph.D. research in 2010. He is also a member of the Institution of Engineers, Australia (IEAust).

Yvonne Tran received the B.Sc. (Hons.) degree in biomedical science and the Ph.D. degree in psychophysiology both from the University of Technology, Sydney, Australia, in 1997 and 2001, respectively.

In 2001, she joined the Centre of Health Technology, University of Technology, Sydney, Australia. In 2007, she joined the Rehabilitation Studies Unit, University of Sydney.

Simon John Geoffrey Lewis is an NHMRC Practitioner Fellow who works as a Consultant Neurologist at the Royal Prince Alfred Hospital and is Associate Professor in Cognitive Neuroscience at the University of Sydney. He is the Director of the Parkinson's Disease Research Clinic at the Brain and Mind Research Institute and heads the NSW Movement Disorders Brain Donor program. He has published over 100 peer review papers exploring various aspects of disease heterogeneity, gait, cognition, sleep, and neuropsychiatry.

Hung Tan Nguyen (SM'06) received the Ph.D. degree from the University of Newcastle, Australia, in 1980.

He is Assistant Deputy Vice-Chancellor (Innovation) at the University of Technology, Sydney, Australia. He is also Director of the Centre for Health Technologies and Professor of Electrical Engineering. His research interests include biomedical engineering, artificial intelligence and image processing, and neurosciences. He has developed biomedical devices for diabetes, neurological disorders, and cardiovascular diseases.

Prof. Dr. Nguyen is a Fellow of the Institution of Engineers, Australia, the British Computer Society, and the Australian Computer Society.